Spatial solitons in periodic Kerr media with fractional diffraction: variational approach

MAHBOUBEH GHALANDARI*
Department of Energy Engineering and Physics, University of Science and Technology of Mazandaran, Behshahr, Iran

The dynamics of spatial solitons in a spatially modulated nonlinear medium are the focus of this research. For the first time, periodic self-focusing effects and fractional diffraction are both incorporated into the wave equation that governs this system. A numerical approach was implemented to resolve the equation, which was derived from the explicit Runge-Kutta method (4,5 order) and the Euler-Lagrange variational principle. Our research concentrates on the impact of oscillations in the nonlinearity strength associated with periodic Kerr self-focusing on the system's critical physical characteristics, including oscillations in peak intensity and changes in soliton width.

(Received March 14, 2025; accepted October 14, 2025)

Keywords: Spatial soliton, Variational approach, Runge-Kutta, Periodic self-focusing

1. Introduction

The equilibrium between linear and nonlinear interactions is the reason that optical solitons keep their shape during traversing [1–3]. A temporal soliton is made when dispersion counteracts with nonlinear effects, which localize the phenomenon in time. In contrast, the soliton becomes spatially confined as a result of spatial soliton, when these effects counteract diffraction [1–3]. The spatial solitons will be the sole focus of this paper. Recently, solitons turn into an interesting subjects in both theoretical and experimental researches in a variety of physics society, such as hydrodynamics, plasma physics, and nonlinear optics, [4,5]. Existence of spatial solitons were predicted in 1964 by Chiao, Garmire, and Townes[6], they showed that in nonlinear media the diffraction-spread of optical beams could be stopped. This feature of spatial solitons was confirmed experimentally too [7–9].

As described in references [10,11] , a novel extension of the Schrödinger equation has been introduced, which is associated with the fractional Hamiltonian. This is clarified in the field of quantum mechanics by the Feynman path integral method, which is applied to Levy flight trajectories and results in the fractional Schrödinger equation (FSE). Although there are some doubts according to the significance of these models [12,13], several experimental results have been suggested to use them in both optical cavity and condensed matter scenarios [14,15].

In order to solve linear and nonlinear time-fractional Schrödinger equations in [16], M. I. Liaqat and A. Akgül advocated a new method. A computational approach was suggested that includes the conformable natural transform and the homotropy perturbation method to generate analytical and numerical solutions for the time-fractional conformable Schrödinger equation, which contains both zero and non-zero entrapping potentials. An iterative algorithm was achieved by Q. Wang and G. Liang [17] to determine sequences of ring and cluster solitons in the (1+2)-dimensional nonlocal nonlinear fractional Schrödinger equation during their investigation of vortex and cluster solitons. They showed that the Lévy index α is a determining factor in the soliton power, orbital angular momentum, and phase rotation period.

A variant array of intriguing dynamic behaviors is expected by the FSE framework, including the dynamics of a Gaussian beam modeled by a fractional Schrödinger equation with a variable coefficient [18], gap solitons in quintic and cubic-quintic fractional nonlinear Schrödinger equations with a periodically modulated linear potential [19], and the restriction of critical collapse of higher-order solitons through the customization of unconventional optical diffraction and nonlinearities [20]. Recently some researchers have shown that a variant of fractional optical solitons can be derived from nonlinear fractional Schrödinger equations (NLFSEs). These include fractional extended nonlinear Schrödinger equation soliton solutions in plasma physics and nonlinear optical fibers[21], a comparative study of new optical solitons of the fractional nonlinear Schrödinger equation with an oscillating nonlinear coefficient [22], new optical soliton solutions for the time-fractional resonant nonlinear Schrödinger equation in optical fibers [23], and conformable time-fractional nonlinear Schrödinger equations for resonant optical solitons [24].

In periodic Kerr media, solitons can exhibit rich dynamics, especially when the diffraction mechanism deviates from the standard second-order model.

In this study, we utilize the variational approach to investigate the nonlinear fractional Schrödinger equation in the presence of periodic Kerr effects. Our primary objective is to investigate the effects of oscillations in the nonlinearity strength that are linked to periodic Kerr self-focusing on the critical physical characteristics of the system, such as oscillations in peak intensity and changes in soliton width.

To contextualize our research, we refer to recent works on fractional diffraction on periodic media [25,26] for the solitons in purely nonlinear lattices , and [27,28] for the solitons in linear lattices.

2. Formalism

The nonlinear Schrödinger equation represents the propagation of spatial solitons, which can be indicated in dimensionless form as follows:

$$i\frac{\partial\psi}{\partial z}=\frac{1}{2}\left(-\frac{\partial^2}{\partial x^2}\right)^{\alpha/2}\psi-g(x)|\psi|^2\psi \quad (1)$$

In this context, ψ shows the slowly varying complex amplitude of the light field, while z and x denote the normalized propagation distance and the normalized transverse coordinate, respectively. The operator $(-\partial^2/\partial x^2)^{\alpha/2}$ is the fractional Laplacian operator in one-dimension, with α representing the Lévy index (where $1<\alpha\leq 2$). In the case where α equals 2, the fractional Schrödinger equation reduces to the familiar standard Schrödinger equation. In equation (1), the first term on the right depends on fractional diffraction, and the second term shows self-focusing (SF). Fractional diffraction refers to the generalization of the diffraction operator to a fractional-order Laplacian, often modeled via the fractional Schrödinger equation. There are several definitions of the fractional Laplacian operator. We use the definition provided in [29].

$$\left(-\frac{\partial^2}{\partial x^2}\right)^{\alpha/2}\psi=\frac{1}{2\pi}\int ds|s|^{\alpha}\int d\xi e^{is(x-\xi)}\psi(\xi) \quad (2)$$

for the one-dimensional case. In this paper, we define the periodic nonlinearity as:

$$g(x)=g_0\cos(x) \quad (3)$$

where g_0 is the strength of the nonlinearity. By using the Lagrangian formulation defined in reference [9], equation (1) can be reformulated as an Euler-Lagrange equation in accordance with the variational principle [16].

$$\delta\int_0^{\infty}\int_{-\infty}^{\infty}\mathcal{L}\left[\psi,\psi^*,\frac{\partial\psi}{\partial z},\frac{\partial\psi^*}{\partial z},\frac{\partial\psi}{\partial x},\frac{\partial\psi^*}{\partial x}\right]dx\,dz=0 \quad (4)$$

where the Lagrangian density $\mathscr{L}$ is equal to:

$$\mathscr{L}=\frac{i}{2}\left(\psi^*\frac{\partial\psi}{\partial z}-\psi\frac{\partial\psi^*}{\partial z}\right)+\frac{g_0\cos(x)}{2}\left(\frac{\partial\psi}{\partial x}\right)\left(\frac{\partial\psi^*}{\partial x}\right)-\frac{1}{2}\psi^2\psi^{*2} \quad (5)$$

We can suggest a trial solution in the Gaussian form:

$$\psi(x,z)=A(z)\,exp\big(ib(z)\big)\,exp\left(-\frac{(1+iq(z))x^2}{4w^2}\right) \quad (6)$$

In this equation, A is the amplitude, b is the phase of the amplitude, w is the beam width and q is the spatial chirp of the beam. By displacing the mentioned trial function into equation (5) and integrating the resulting expression with respect to x, the reduced variational problem is achieved.

$$\delta\int_0^{\infty}\mathscr{L}\,dz=0 \quad (7)$$

where $L=\int_{-\infty}^{\infty}\mathcal{L}\,dx$ is the Lagrangian. Then by doing some calculations, the average value $\langle L\rangle$ can be ascertained analytically.

$$\langle L\rangle=-\sqrt{\pi}\,\mathrm{A}(z)^2\,w(z)\,b'(z)+\frac{1}{2}\sqrt{\frac{\pi}{2}}\,\mathrm{g0}\,\mathrm{A}(z)^4\,e^{-\frac{1}{8}\mathrm{w}(z)^2}\,w(z)+\frac{1}{4}\sqrt{\pi}\,\mathrm{A}(z)^2\,w(z)\,q'(z)$$
$$-\frac{1}{2}\sqrt{\pi}\,\mathrm{A}(z)^2\,q(z)\,w'(z)-\frac{1}{2}\Gamma\left(\frac{\alpha+1}{2}\right)\mathrm{A}(z)^2\,(\mathrm{q}(z)^2+1)^{\alpha/2}\,\mathrm{w}(z)^{1-\alpha} \quad (8)$$

Here, $\Gamma\left(\frac{\alpha+1}{2}\right)$ is the gamma function. By applying the Lagrangian $\langle L\rangle$, we then get a set of variational equations that govern the Gaussian parameters $p_j(z)$ (where j=1,23,4).

$$\frac{d}{dz}\left(\frac{\partial L}{\partial\dot{p}_j}\right)-\frac{\partial L}{\partial p_j}=0 \quad (9)$$

where $P_j=dP_j/dz$. After a upright calculation, we get the below equations:

$$A'(z)=\frac{\alpha\Gamma\left(\frac{\alpha+1}{2}\right)A(z)q(z)(q(z)^2+1)^{\frac{\alpha}{2}-1}w(z)^{-\alpha}}{2\sqrt{\pi}} \quad (10)$$

$$w'(z)=-\frac{\alpha\Gamma\left(\frac{\alpha+1}{2}\right)q(z)(q(z)^2+1)^{\frac{\alpha}{2}-1}w(z)^{1-\alpha}}{\sqrt{\pi}} \quad (11)$$

$$q'(z)=\frac{\mathrm{g0}A(z)^2e^{-\frac{1}{8}w(z)^2}w(z)^2}{4\sqrt{2}}+\frac{\mathrm{g0}A(z)^2e^{-\frac{1}{8}w(z)^2}}{\sqrt{2}}-\frac{\alpha\Gamma\left(\frac{\alpha+1}{2}\right)(q(z)^2+1)^{\alpha/2}w(z)^{-\alpha}}{\sqrt{\pi}} \quad (12)$$

$$b'(z) = \frac{5g0A\,(z)^2 e^{-\frac{1}{8}w\,(z)^2}}{4\sqrt{2}(q\,(z)^2+1)} + \frac{5g0A\,(z)^2 q\,(z)^2 e^{-\frac{1}{8}w\,(z)^2}}{4\sqrt{2}(q\,(z)^2+1)} + \frac{g0A\,(z)^2 e^{-\frac{1}{8}w\,(z)^2} w\,(z)^2}{16\sqrt{2}(q\,(z)^2+1)} + \frac{g0A\,(z)^2 q\,(z)^2 e^{-\frac{1}{8}w\,(z)^2} w\,(z)^2}{16\sqrt{2}(q\,(z)^2+1)}$$
$$+ \frac{\alpha\Gamma\,(\frac{\alpha+1}{2}) q\,(z)^2 (q\,(z)^2+1)^{\frac{\alpha}{2}-1} w\,(z)^{-\alpha}}{4\sqrt{\pi}} - \frac{\Gamma\,(\frac{\alpha+1}{2}) q\,(z)^2 (q\,(z)^2+1)^{\frac{\alpha}{2}-1} w\,(z)^{-\alpha}}{2\sqrt{\pi}}$$
$$- \frac{\alpha\Gamma\,(\frac{\alpha+1}{2})(q\,(z)^2+1)^{\frac{\alpha}{2}-1} w\,(z)^{-\alpha}}{4\sqrt{\pi}} - \frac{\Gamma\,(\frac{\alpha+1}{2})(q\,(z)^2+1)^{\frac{\alpha}{2}-1} w\,(z)^{-\alpha}}{2\sqrt{\pi}} \tag{13}$$

By solving Eqs. (10) to (13) and using the explicit Runge-Kutta (4,5) numerical method with the initial conditions A(0)=1, w (0) = 1, q (0) = 0, b(0)=1. The numerical results will be introduced in the next section.

3. Results and discussion

The on-axis intensity of the soliton is shown in Fig. 1 as a function of the normalized propagation distance z for a constant nonlinearity strength g_0=1 and various Lévy indices α=1.2, 1.5, 1.8.

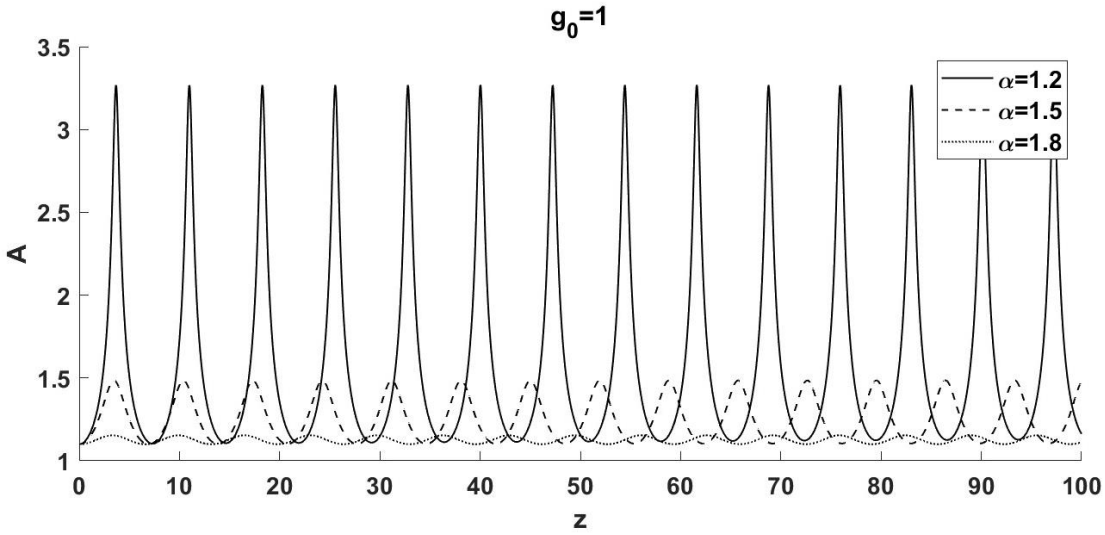

Fig. 1. The changes in the on-axis intensity of soliton as a function of the normalized propagation distance z. The nonlinearity strength g_0=1 is fixed, and the Lévy index α is varied between 1.2, 1.5, and 1.8

The intensity of the soliton's on-axis decreases specifically when the Lévy index α changes from 1.2 to 1.5. This shows that the maximal intensity of the soliton is decreased as the Lévy indices enhance. The slowing ratio for intensity decreasing is from α = 1.5 to α = 1.8, showing that the intensity fixates more as α keep going to enhance. As the Lévy index enhances from 1.2 to 1.8, the number of oscillations in the on-axis intensity of the soliton also enhances. This proves that the dynamics of larger Lévy indices are more complex, resulting in greater oscillations in intensity along the propagation distance z. As a result, the conduct illustrated in Fig. 1 can be defined as follows: The soliton conserves a comparatively high peak intensity with fewer oscillations at α=1.2. The intensity of the soliton decreases much more, and oscillations stay more pronounced at α=1.5. At α=1.8, the soliton feels a delayed decline in intensity, but the number of oscillations enhance further. This offers that the Lévy index is a critical factor in the dynamics of the soliton, as it affects the amplitude and oscillatory behavior of its intensity profile.

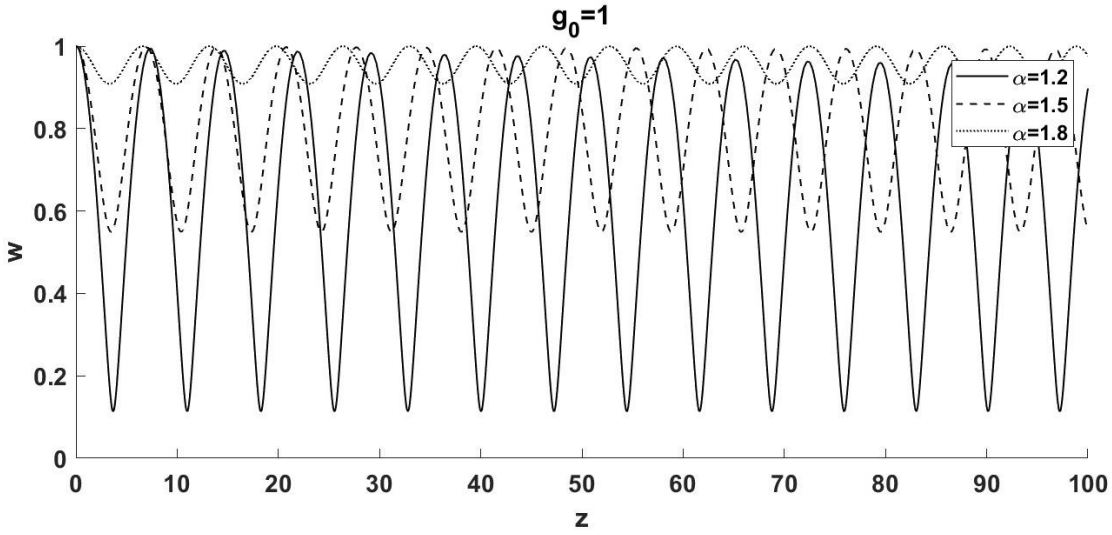

Fig. 2. The changes in the width of soliton as a function of the normalized propagation distance z. The nonlinearity strength g_0=1 is fixed, and the Lévy index α is varied between 1.2, 1.5, and 1.8

Fig. 2 shows the relation between the soliton width and the normalized propagation distance z for a nonlinearity strength of g_0=1 and various Levy indices α=1.2,1.5,1.8. It is clear that the laser spot size indicates oscillations that resemble a sine wave. The average value stays constant when these oscillations happen around the z-axis. As shown in Fig. 2, soliton-like behavior is seen for a variety of Levy indices, and all solitons stay stable within the limited area of 1.2<α<1.8. Moreover, the number of soliton width oscillations increases as the Levy index enhances, as well as the amplitude of these oscillations decreases.

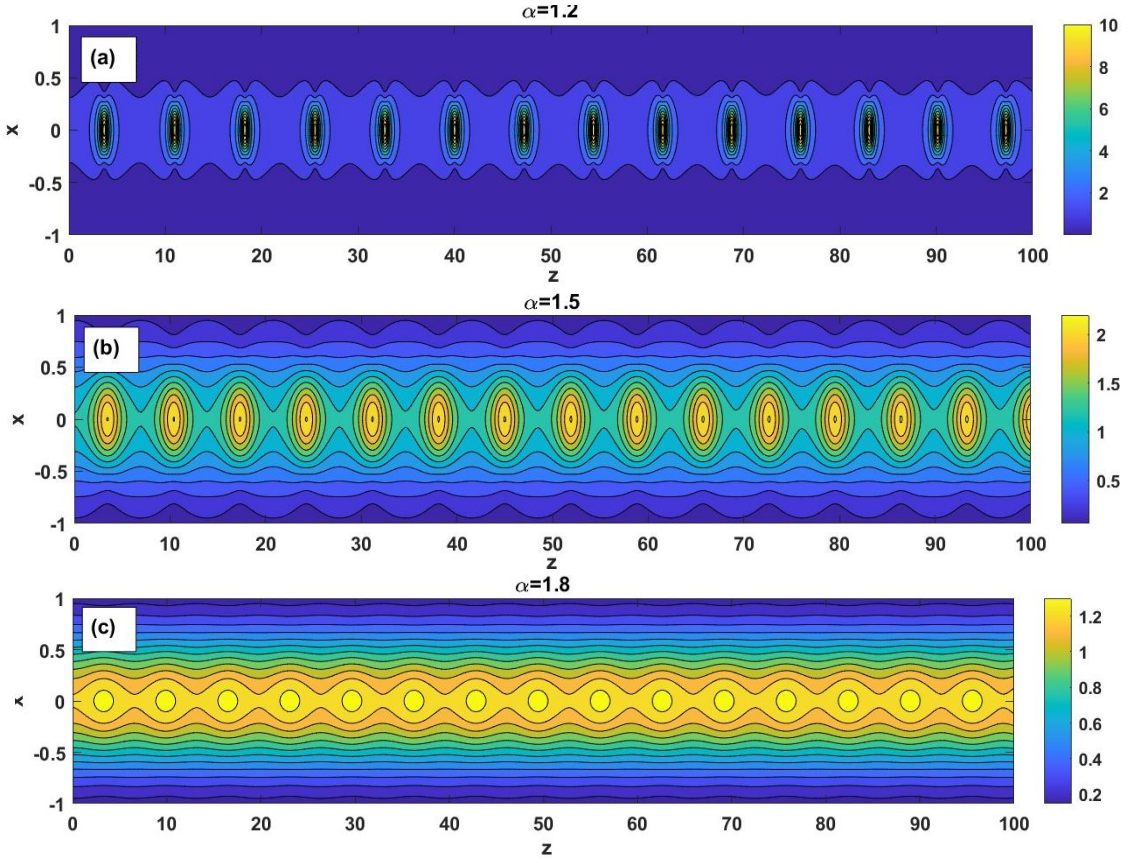

Fig. 3. The simulations of soliton propagation in a waveguide with nonlinearity strength g_0=1 are conducted for a variety of Lévy indices, including (a) α=1.2, (b) α=1.5, and (c) α=1.8 (colour online)

Fig. 3 shows contour graphs that represent the intensity of a soliton which propagates through a waveguide with a nonlinearity strength of g_0= 1. These diagrams are represented for different Lévy indices, including (a) α = 1.2, (b) α = 1.5, and (c) α = 1.8. The Lévy index α is an important factor of the oscillation period of the soliton, as achieved by the numerical analysis. When the value of α enhances from 1.2 to 1.8, the oscillation period decreases, and this process leads to faster oscillations. Besides, the peak intensity of the soliton decreases as α enhances, while its spatial breadth enhances, suggesting a broader soliton profile at higher Lévy indices.

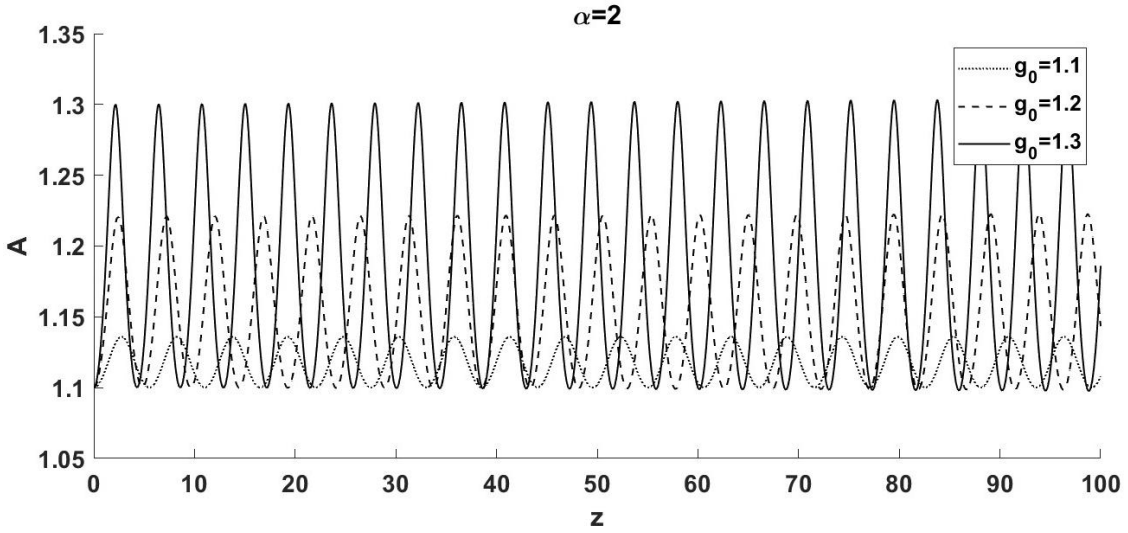

*Fig. 4. The changes in the width of soliton as a function of the normalized propagation distance z. The Lévy index α =2 is fixed, and the nonlinearity strength g_0 is varied between 1.1, 1.2, and 1.*3

Fig. 4 shows the oscillations in soliton width and on-axis intensity as a function of the normalized propagation distance z, with a Levy index α=2 for different values of nonlinearity strength g_0 =1.1, 1.2, 1.3. As demonstrated in Fig. 4, the soliton's on-axis intensity oscillates at a higher amplitude and the number of oscillations enhances as the nonlinearity strength is enhanced from g_0=1.1 to g_0=1.3. This progress proves that the soliton experiences more frequent and intense oscillations as the nonlinearity strength enhances. The amplitude enhancement is declarative of the soliton's intensity oscillations being more pronounced, while the enhanced number of oscillations offers that the soliton's features are deriving at a quicker pace along the propagation distance. Such a behavior confirms the direct correlation between nonlinearity and soliton dynamics, as the oscillatory behavior of the soliton can be specially changed by modifying the intensity of the nonlinearity.

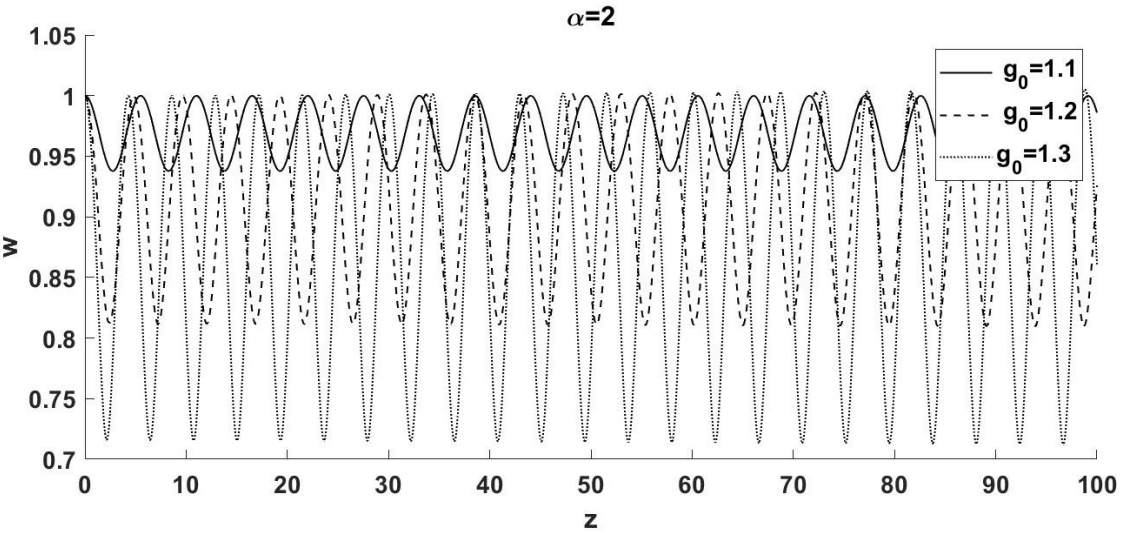

Fig. 5. The changes in the on-axis intensity of soliton as a function of the normalized propagation distance z. The Lévy index α =2 is fixed, and the nonlinearity strength g_0 is varied between 1.1, 1.2, and 1.3

The changes in soliton width relative to the normalized propagation distance z for different values of nonlinearity strength, specifically g_0 = 1.1,1.2,1.3, as shown in Fig. 5. The laser beam size exposes a sine-like oscillation pattern, as suggested by the diagram. The average value stays constant throughout these oscillations, which vary around the z-axis. The soliton affirms conventional soliton-like behavior for a different kind of nonlinearity strengths, as shown in the Fig. 5. Moreover, the number of oscillations in the soliton's width enhances when the nonlinearity strength is enhanced. On the other hand, the amplitude of these oscillations enhances, representing that the intensity of the nonlinearity influences both the frequency and the size of the width oscillations. This finding emphasizes that the nonlinearity in the system and the oscillatory behavior of the soliton is directly related to each other. Not only do the oscillations in width are more frequent when the nonlinearity is stronger, but their amplitude also enhances, offering a more pronounced fluctuation in the soliton's size within propagation.

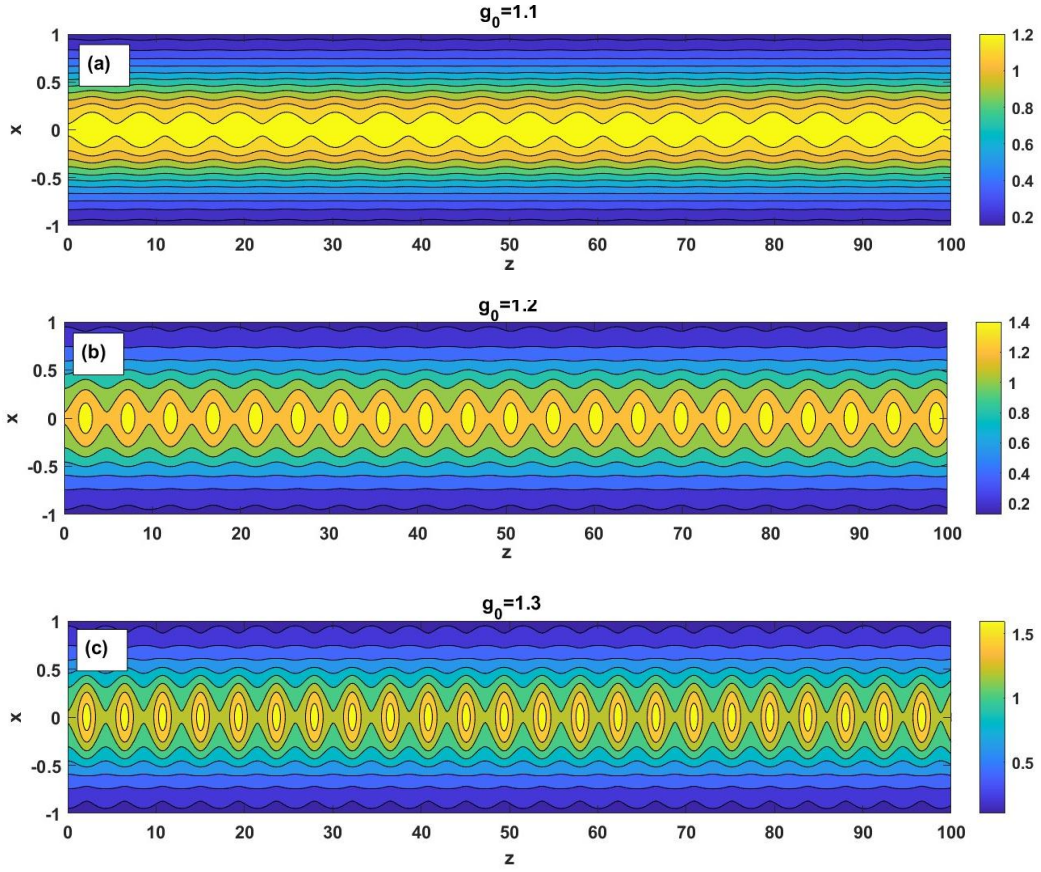

Fig. 6. Numerical simulations of soliton propagation in a waveguide with a Lévy index of α=2 for various nonlinearity strengths. The simulations include (a) g_0 =1.1, (b) g_0=1.2, and (c) g_0=1.3 (colour online)

Contour diagrams are illustrated in Fig. 6, which show the intensity of a soliton as it propagates through a waveguide with a Levy index of α=2, while the nonlinearity strength is different. The plots correspond to three obvious values: (a) g_0 = 1.1, (b) g_0= 1.2, and (c) g_0= 1.3. Varieties in the nonlinearity strength g_0 affect the behavior of the soliton in these computations, which is constant with the patterns showed in Fig. 3. The oscillation period of the soliton decreases as the nonlinearity strength g_0 enhances from 1.1 to 1.3, leading to more quick oscillations. Nevertheless, the maximal intensity of the soliton increases in tandem with the strength of the nonlinearity, instead to the oscillation period. It is intriguing that the soliton's width remains constant, exhibiting no discernible variation, despite the variations in oscillation period and intensity.

4. Conclusions

In summary, the propagation of solitons in a spatially modulated fractional system has been examined. Soliton-like behavior was seen for a different kind of Lévy indices. The number of oscillations in the soliton width enhanced when the Lévy index enhanced, while the amplitude of these oscillations decreased. Furthermore, the number of oscillations in the soliton's width enhanced, and the amplitude of these oscillations are more pronounced, as the nonlinearity strength g_0 enhanced. As the Lévy index α

enhanced, the oscillation period decreased. Additionally, we understood that the soliton's spatial extent expanded as α increased, while its maximal intensity decreased.

References

[1] G. P. Agrawal, Nonlinear Science at the Dawn of the 21st Century, Springer, 195 (2000).
[2] G. P. Agrawal, Fiber-Optic Communication Systems, John Wiley & Sons, 2012.
[3] S. Trillo, W. Torruellas, Spatial Solitons, Springer, 2013.
[4] N. N. Akhmediev, A. Ankiewicz, Nonlinear Pulses and Beams, Springer, 1997.
[5] Y. S. Kivshar, G. P. Agrawal, Optical Solitons: From Fibers to Photonic Crystals, Academic Press, 2003.
[6] R. Y. Chiao, E. Garmire, C. H. Townes, Phys. Rev. Lett. **13**, 479 (1964).
[7] J. S. Aitchison, Y. Silberberg, A. M. Weiner, D. E. Leaird, M. K. Oliver, J. L. Jackel, E. M. Vogel, P. W. E. Smith, Journal of the Optical Society of America B **8**, 1290 (1991).
[8] J. S. Aitchison, A. M. Weiner, Y. Silberberg, D. E. Leaird, M. K. Oliver, J. L. Jackel, P. W. E. Smith, Opt. Lett. **16**, 15 (1991).
[9] A. Barthelemy, S. Maneuf, C. Froehly, Opt. Commun. **55**, 201 (1985).
[10] N. Laskin, Phys. Rev. E **62**, 3135 (2000).
[11] N. Laskin, Phys. Rev. E **66**, 56108 (2002).
[12] Y. Wei, Phys. Rev. E **93**, 66103 (2016).
[13] N. Laskin, Phys. Rev. E **93**, 66104 (2016).
[14] B. A. Stickler, Phys. Rev. E - Statistical, Nonlinear, Soft Matter Phys. **88**, 12120 (2013).
[15] S. Longhi, Opt. Lett. **40**, 1117 (2015).
[16] M. I. Liaqat, A. Akgül, Chaos, Solitons and Fractals **162**, 112487 (2022).
[17] Q. Wang, G. Liang, J. Opt. **22**, 55501 (2020).
[18] F. Zang, Y. Wang, L. Li, Opt. Express **26**, 23740 (2018).
[19] L. Zeng, J. Zeng, Nonlinear Dyn. **98**, 985 (2019).
[20] L. Zeng, J. Zeng, Commun. Phys. **3**, 26 (2020).
[21] J. Ahmad, S. Akram, K. Noor, M. Nadeem, A. Bucur, Y. Alsayaad, Sci. Rep. **13**, 10877 (2023).
[22] M. B. Riaz, A. Atangana, A. Jahngeer, F. Jarad, J. Awrejcewicz, Results Phys. **37**, 105471 (2022).
[23] N. Das, S. Saha Ray, Opt. Quantum Electron. **54**, 112 (2022).
[24] A. R. Seadawy, M. Bilal, M. Younis, S. T. R. Rizvi, Int. J. Mod. Phys. B **35**, 2150044 (2021).
[25] L. Zeng, J. Zeng, Opt. Lett. **44**, 2661 (2019).
[26] L. Zeng, D. Mihalache, B. A. Malomed, X. Lu, Y. Cai, Q. Zhu, J. Li, Chaos, Solitons & Fractals **144**, 110589 (2021).
[27] X. Zhu, M. R. Belić, D. Mihalache, D. Cao, L. Zeng, Physica D Nonlinear Phenomena **470**, 134379 (2024).
[28] X. Zhu, M. R. Belić, D. Mihalache, D. Xiang, L. Zeng, Opt. Laser Technol. **184**, 112426 (2025).
[29] X. Zhu, M. R. Belić, D. Mihalache, D. Xiang, L. Zeng, Eur. Phys. J. Plus **139**, 1116 (2024).

*Corresponding author: mahboubeh.ghalandari@gmail.com; m.ghalandari@mazust.ac.ir